

## CROSS-SECTIONAL FAILURE CRITERION COMBINED WITH STRAIN-HARDENING DAMAGE MODEL FOR SIMULATION OF THIN-WALLED TEXTILE-REINFORCED CONCRETE SHELLS

Sharei E.<sup>1</sup>, Chudoba R.<sup>1</sup>, and Scholzen A.<sup>1</sup>

<sup>1</sup>Institute of Structural Concrete - RWTH Aachen University  
Mies-van-der-Rohe-Str. 1  
52074 Aachen, Germany  
e-mail: esharei@imb.rwth-aachen.de

**Keywords:** Textile reinforced concrete, Cementitious composites, Damage mechanics, Shell structures, Failure criterion, Finite element analysis

**Abstract.** *Application of textile reinforced concrete (TRC) can significantly facilitate the manufacturing of thin-walled shell structures. Thanks to the high tensile strength and longtime durability of textile reinforcement, construction of much thinner cross sections compared to ordinary reinforced concrete has become possible. Furthermore the form-flexibility of textile reinforcement allows for much more freedom in design of shells with more complex geometries. However, these advantages make the prediction of the structural behavior under imposed loads much more difficult. Due to the complex stress redistribution in the plane of shell and also the anisotropic behavior of the composite material, different modes of failure can be observed in TRC shell structures. In this paper we focus on the failure criterion of thin-walled TRC shell elements. In particular, we propose a criterion reflecting the interaction of normal force and bending moment in a shell cross section. The failure criterion has been implemented in combination with an anisotropic damaged-based material model in order to provide realistic prediction of the structural load-carrying behavior. The accuracy of the model in prediction of different failure modes has been validated using three different types of tests setups.*

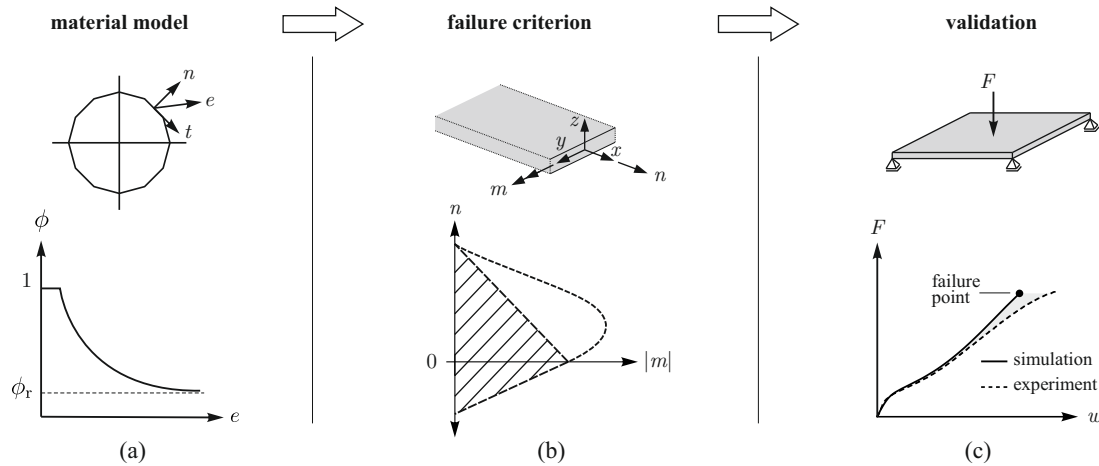


Figure 1: (a) material model formulation; (b) failure criterion of the TRC cross section based on  $n$ - $m$  interaction diagram; (c) validation of the failure criterion based on laboratory tests

## 1 INTRODUCTION

Textile reinforced concrete (TRC) is a composite material consisting of high performance fine aggregate matrix reinforced with textile reinforcement made of carbon or alkali-resistant glass rovings in form of fabrics. Two important characteristics of textile reinforcement are non-corrosiveness and high tensile strength. Application of this type of reinforcement increases the durability of the composite material compared to steel reinforced concrete and extends the range of its applicability in construction. Recently, TRC has been used for construction of large scale, thin-walled shells [1, 2], sandwich wall or slab panels [3], facade elements [4] and pedestrian bridges [5]. Focus of this paper is restricted to thin-walled TRC shell structures uniformly reinforced with textile fabrics.

TRC shell elements exhibit a complex behavior in terms of nonlinearity and anisotropy imposed to *in-plane* and *out-of-plane* loading conditions. Interaction of textile reinforcement with concrete matrix leads to multiple cracking under tension. Therefore, nonlinear behavior of strain-hardening type is observed in the composite material. Anisotropic behavior of TRC is due to the formation of cracks perpendicular to the principle direction of stresses [6]. At a macroscopic level, the process of crack pattern development can be viewed and modeled using *anisotropic damage* model.

In this paper behavior of the TRC shells at the material level and structural level has been investigated with the goal to formulate both realistic and pragmatic failure criterion. The overview of the modeling framework is shown in Fig. 1. In Section 2 the modeling approach with a brief description of the material model is presented. Consequently, after a brief description of calibration and validation of the model in Section 3 based on the previous studies, we investigate the failure criterion for TRC elements exposed to combined tensile force and bending moment in Section 4. The feasibility of the cross-sectional failure criterion has been demonstrated by calibrating the material model and the failure criterion using *tensile test*, *compressive test*, *bending test*. The validation for combined tensile and bending loads was performed using a *slab test*.

## 2 MODELING APPROACH OF TRC SHELLS

The crack pattern in the studied type of composite structures is fine in relation to the dimensions of the structural elements. This fine nature of cracking justifies a smeared representation

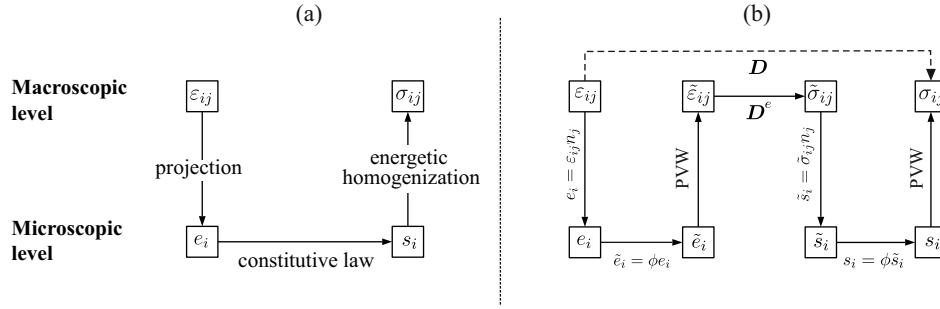


Figure 2: (a) basic principle of microplane model; (b) constitutive stress-strain relation in microplane damage model

of cracking using a homogenized strain-hardening model. In order to capture the nonlinearity and anisotropy of TRC, a damage-based model of microplane type has been used. Material models with microplane approach are generally characterized as a constitutive relation between the strain and stress on plane of various orientations, so called *microplanes* [7]. Evolution of damage on a microplane is governed by a damage function. The shape of damage function can be tailored for either quasi-brittle materials with strain-softening behavior, e.g. plain concrete [8], or it can also reproduce the strain hardening behavior of quasi-ductile materials such as TRC [9].

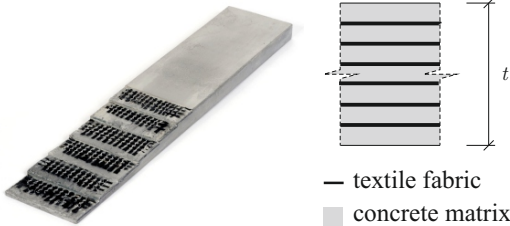
Basic structure of microplane model approach is shown in Fig. 2a. The constitutive mapping of strain to stress is done in three steps: (i) geometric projection of macroscopic strain tensor  $\varepsilon_{ij}$  into microplane directions providing strain vectors  $e_i$ , (ii) application of constitutive law between strain vector  $e_i$  and stress vector  $s_i$ , (iii) energetic homogenization of microplane stress vectors based on the principle of virtual work (PVW) to obtain the global stress tensor  $\sigma_{ij}$ . The damage-based form of microplane model (microplane damage model) has been presented by Jirásek [8]. Constitutive formulation of this model is shown in Fig. 2b. In this formulation, the mapping of apparent strain/stress vectors ( $e_i$  and  $s_i$ ) to the effective strain/stress vectors ( $\tilde{e}_i$  and  $\tilde{s}_i$ ) is done on a microplane level using a damage function  $\phi$ . Inverse transformation of the variables from the microplane level to the macroscopic level is performed by principle of virtual work (PVW), setting the summation of virtual works of the forces applied to the system (in microscopic and macroscopic level) equal to zero. Although there is an explicit relation between effective strain and stress tensors ( $\tilde{\varepsilon}_i$  and  $\tilde{\sigma}_i$ ) in terms of elastic stiffness tensor  $D^e$ , the global strain to stress mapping is only possible by consecutive steps of projection and energetic homogenization between macroscale and microplane levels to generate the stiffness tensor in damaged state  $D$ .

For the purpose of modeling of TRC shell structures, a two-dimensional formulation of the microplane damage model with strain-hardening for TRC has been presented by the authors in [10]. By means of dimensional reduction of the model, microplane damage model is used only for strain and stress components in the in-plane directions of the TRC shell and material behavior along the thickness of the shell is assumed to be linear elastic.

### 3 CALIBRATION AND VALIDATION

In order to determine the shape of the damage function of a certain TRC cross section, the material model needs to be calibrated. A direct incremental calibration procedure by means of a tensile test on a TRC specimen has been presented by Scholzen et al. [9]. The capability of the calibrated model in prediction of structural behavior of a large scale TRC shell has been

Table 1: Properties of TRC cross section

description	symbol	value	unit	cross section layout
width	$b$	100	mm	
thickness	$t$	20	mm	
total cross section	$A$	2000	mm <sup>2</sup>	
number of textile layers	$n_{\text{tex}}$	6	—	
textile cross section	$A_{\text{tex}}$	32.1	mm <sup>2</sup>	
reinforcement ratio	$\rho_{\text{tex}}$	1.61	%	

presented by Sharei et al. [11].

The calibration is exemplified for TRC tensile test specimens reinforced with 6 equidistant layers non-impregnated carbon fabrics. Cross section properties and reinforcement layout within the cross section is given in Table. 1. The test setup with the specimen of the length  $l = 1000$  mm is shown in Fig. 3a. Strain has been measured within the length of  $l_m = 250$  mm. Stress-strain curve of the tensile test is given in Fig. 3b. The maximum tensile strain achieved in the test was  $\varepsilon_f = 7.05$  ‰. Calibration of the material for this cross section based on [9] leads to the damage function in Fig. 3c. Failure assessment of laboratory tests has been performed by implementing the material model and the failure criterion in the finite element code ABAQUS[12].

During tensile test, damage evolves in form of a finely spaced cracks oriented perpendicularly to the direction of the tensile force. The failure occurs in the weakest crack once the ultimate strength of the textile reinforcement is achieved. The calibrated damage function represents the failure as a drop of the integrity value to zero. Thus, the tensile test serves for the calibration of the nonlinear behavior during the matrix cracking and, at the same time, for the identification of the ultimate failure.

#### 4 CROSS-SECTIONAL FAILURE CRITERION

It is well known, that the bending tensile strength (also called as modulus of rupture) of quasi-brittle materials is larger than the tensile strength measured in tensile test [13]. In case of TRC, two major sources of the difference between tensile strength in pure tension and in bending can be specified distinguished:

- *Statistical size-effect*: In the tensile tests many crack bridges along the tested zone develop with weakest one defining the ultimate failure. In the three-point bending test, only the cross section at mid-span is actually tested, which may not be the weakest one.
- *Tensile load transfer*: Even for very smooth transfer of tensile load into the tensile specimen, local stress concentrations in the vicinity of clamps cannot be completely avoided and cause a premature specimen failure.

In order to properly reflect the macroscopically observed strength of a shell cross section, we propose a strength criterion defined at the level of the stress resultants of a cross section. In principle, the same approach is used in usual dimensioning approaches. In our case, we built the criterion on top of the material model implementation. Thus, except of the standard mapping



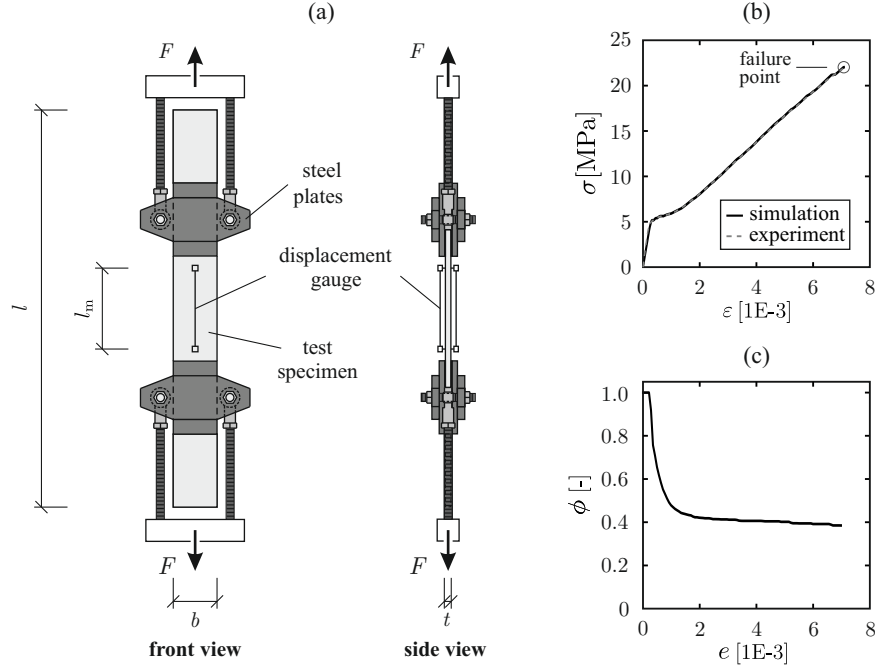


Figure 3: (a) test setup of pure tensile test; (b) stress-strain curve of the tensile test; (c) calibrated damage function

between the strain to stress tensors within an iteration loop, the material model also evaluates the stress resultants for a shell cross section and checks the level of its utilization.

In order to implement the cross-sectional criterion, the first step is to extend the strain capacity in the damage function beyond the limit measured in the tensile test given in Fig. 3c. Furthermore, the cross-sectional stress resultants, i.e. the vectors of normal forces  $n$  and bending moments  $m$  are calculated for each integration point of a shell. For a cross section depicted in Fig. 1b, normal force  $n$  and bending moment  $m$  are determined during the analysis by integrating the stresses in the TRC cross section as:

$$n = \int_t \sigma_x dz \quad m = \int_t z \sigma_x dz \quad (1)$$

The cross-sectional resistance in presence of both normal force and bending moment is defined as a failure envelope shown in Fig. 4a. The real and the simplified  $n$ - $m$  envelope of a TRC cross section includes the values of strength in pure tension ( $n_{t,Rm}$ ), compression ( $n_{c,Rm}$ ) and bending ( $m_{Rm}$ ) [2]. Simplification of the failure envelope using the linear interpolation has been justified using a tests series on TRC specimens loaded with combined tensile force and bending moment [14]. The normalized form of the envelope is shown in Fig. 4b defining the utilization parameters as:

$$\eta_{nt} = \frac{n}{n_{t,Rm}} \quad \eta_{nc} = \frac{-n}{n_{c,Rm}} \quad \eta_m = \frac{|m|}{m_{Rm}}. \quad (2)$$

Utilization ratio  $\eta_{nm}$  of the cross section can be evaluated as:

$$\eta_{nm} = \max \{ \eta_{nc}, \eta_{nt} \} + \eta_m. \quad (3)$$

Failure in a TRC cross section occurs once the interaction of normal force  $n$  and bending moment  $m$  exceeds the admissible range of  $n$ - $m$  envelope in Fig. 4, or in the normalized form:

$$\eta_{nm} > 1. \quad (4)$$

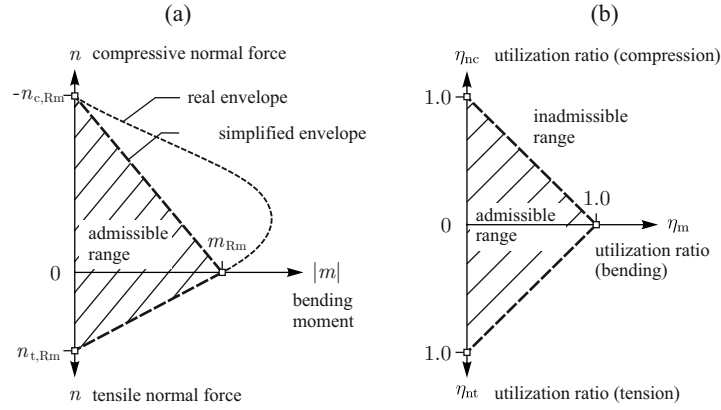


Figure 4: Failure envelope of TRC cross section based on (a)  $n$ - $m$  interaction diagram and (b)  $\eta_n$ - $\eta_m$  interaction diagram

Strength characteristics of the TRC cross section in Table. 1 have been determined as: tensile strength  $n_{t,Rm} = 476$  N/mm, compressive strength  $n_{c,Rm} = 1666.7$  N/mm and bending strength  $m_{Rm} = 3330$  Nmm/mm.

The force-deflection curves measured and simulated for three-point bending test on a TRC specimen with the span length of  $l = 460$  mm and the cross section given in Table. 1 is shown in Fig. 5a. Test has been performed with three repetitions. As indicated in Fig. 5a, the tensile strength determined in tensile test is attained at  $\approx 70$  % of the ultimate force in three-point bending test. Stress and strain cross-sectional profiles corresponding to the failure point are given in Fig. 5b with failure tensile strain of  $1.66$  ‰ is beyond the ultimate tensile strain in the tensile test.

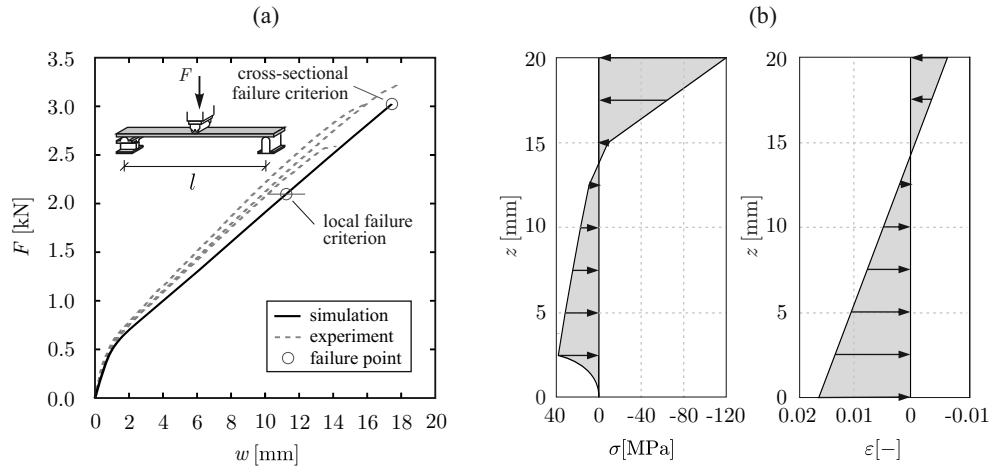


Figure 5: (a) Comparison of load-displacement curves and ultimate failure of TRC bending tests for test and simulation applying two failure criteria; (b) stress and strain profiles in the cross section at failure

The validation of the cross-sectional failure criterion for prediction of the structural behavior including stress redistribution and complex damage pattern has been performed using TRC slab test. Test specimen had dimensions of  $800 \times 800$  mm with the cross section parameters given in Table 1. The pin supported specimen was loaded at the center using displacement control as shown in Fig. 6. Simulation of the slab test was performed with and without consideration of

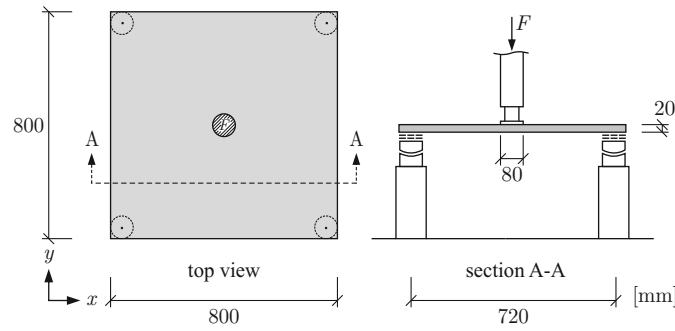


Figure 6: Test setup of the slab test

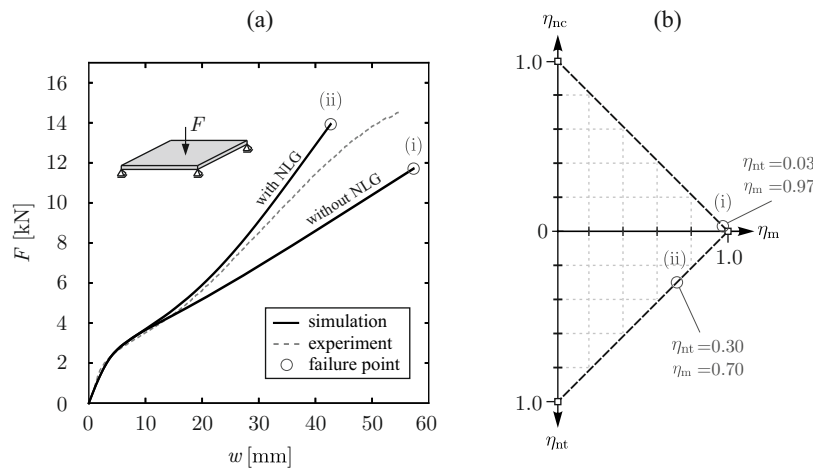


Figure 7: (a) Comparison of force-deflection curves and ultimate failure of TRC slab test for test and simulation applying cross-sectional failure criterion; (b) corresponding utilization ratios in the  $\eta_n$ - $\eta_m$  interaction diagram with and without consideration of geometrical nonlinearity

geometrical nonlinearity. Since the deflection of the slab was large, membrane effect could be activated during the later stages of loading. In this way, the ultimate failure was achieved for combined action of tensile force and bending moment. The geometrically linear model without the ability to reflect the membrane effect resulted in unrealistic prediction of the true behavior (force-deflection curve labeled *without NLG* in Fig. 7a). The corresponding utilization ratios are  $\eta_n = 0.03$  and  $\eta_m = 0.97$  for tensile force and bending moment respectively as shown in Fig. 7b, indicating a pure bending failure without activation of membrane forces in the cross section.

The force-deflection curve with the considered effect of geometrical nonlinearity, (labeled *with NLG* in Fig. 7a), has revealed a membrane effect leading to a failure with utilization ratios for tensile force and bending moment of  $\eta_n = 0.30$  and  $\eta_m = 0.70$ , respectively as depicted in Fig. 7b, indicating a considerable tensile force in the cross section at failure. The corresponding  $n$ - $m$  pairs for both cases with and without geometrical nonlinearity are given in Table 2.

## 5 CONCLUSIONS

In this study failure of thin-walled TRC shell structures imposed to in-plane and out-of-plane loading conditions was investigated. Failure was predicted using two approaches: 1) local failure criterion (failure of material point) and 2) cross-sectional failure criterion (failure through  $n$ - $m$  interaction). Based on the simulation results we can conclude that the cross-

Table 2: Assessment of the  $n$ - $m$  failure criterion for the slab tests with and without consideration of geometrical nonlinearity (NLG)

NLG	$n$	$m$	$\eta_{nc}$	$\eta_{nt}$	$\eta_m$
	[N/mm]	[Nmm/mm]	[—]	[—]	[—]
without	-46	-3246	0.03	-	0.97
with	143	-2350	-	0.30	0.70

sectional failure criterion can effectively represent the stress redistribution effects within a TRC cross section and provides a realistic estimate of the ultimate structural load.

## ACKNOWLEDGEMENTS

The financial support by *Deutsche Forschungsgemeinschaft (DFG)* (project No. 276/2-2) is gratefully acknowledged.

## REFERENCES

- [1] Scholzen A., Chudoba R., and Hegger J. Thin-walled shell structure made of Textile Reinforced Concrete; Part I: structural design and construction. *Structural Concrete*, 16:106–114, 2015.
- [2] Scholzen A., Chudoba R., and Hegger J. Thin-walled shell structure made of Textile Reinforced Concrete; Part II: experimental characterization, ultimate limit state assessment and numerical simulation. *Structural Concrete*, 16:115–124, 2015.
- [3] Shams A., Horstmann M., and Hegger J. Experimental investigations on Textile-Reinforced Concrete (TRC) sandwich sections. *Composite Structures*, 118:643–653, December 2014.
- [4] Hegger J., Kulas C., and Horstmann M. Spatial textile reinforcement structures for ventilated and sandwich facade elements. *Advances in Structural Engineering*, 15(4):665–676, April 2012.
- [5] Hegger J., Goralski C., and Kulas C. A slender pedestrian bridge made of textile reinforced concrete. *International Association for Bridge and Structural Engineering (IABSE)*, Venice, Italy, September 2010.
- [6] Hughes B. P. and Ash J. E. Anisotropy and failure criteria for concrete. *Materiaux et Construction*, 3(6):371–374, November 1970.
- [7] Bažant Z. P. and Prat P. C. Microplane model for brittle-plastic material: I. Theory. *Journal of Engineering Mechanics*, 114(10):1672–1688, 1988.
- [8] Jirásek M. Comments on microplane theory. *Mechanics of Quasibrittle Materials and Structures*, Hermes Science Publications, pages 55–77, 1999.
- [9] Scholzen A., Chudoba R., and Hegger J. Calibration and validation of a microplane damage model for cement-based composites applied to Textile Reinforced Concrete. In Barros H., Faria C., and Ferreira C., editors, *International Conference on Recent Advances*

- in Nonlinear Models - Structural Concrete Applications (CoRAN 2011)*, pages 417–427. ECCOMAS Thematic Conference, November 2011.
- [10] Sharei E., Scholzen A., Chudoba R., and Hegger J. Anisotropic damage model for numerical simulation of Textile Reinforced Concrete shell structures. In Topping B.H.V. and Iványi P., editors, *Twelfth International Conference on Computational Structures Technology (CST 2014)*. Civil-Comp Press, September 2014.
- [11] Sharei E., Scholzen A., and Chudoba R. Nonlinear analysis of textile reinforced concrete shells using an anisotropic, damaged-based material model. In Brameshuber W., editor, *11th International Symposium on Ferrocement (FERRO-11) and 3rd International Conference on Textile Reinforced Concrete (ICTRC-3)*, pages 133–139. RILEM Publications S.A.R.L., June 2015.
- [12] Dassault Systèmes Simulia Corp., Providence, RI, USA. *ABAQUS User Subroutines Reference Manual, Version 6.11*, 2011.
- [13] Troxell G. E., Harmer E. D., and Joe W. K. *Composition and Properties of Concrete*. McGraw Hill, second edition, 1968.
- [14] Scholzen A., Chudoba R., and Hegger J. Ultimate limit state assessment of TRC structures with combined normal and bending loading. In Brameshuber W., editor, *11th International Symposium on Ferrocement (FERRO-11) and 3rd International Conference on Textile Reinforced Concrete (ICTRC-3)*, pages 159–166. RILEM Publications S.A.R.L., June 2015.